2014 IEEE International Conference on Robotics & Automation (ICRA)
Hong Kong Convention and Exhibition Center
May 31 - June 7, 2014. Hong Kong, China

Robot design for bidirectional locomotion induced by vibration excitation

Jaeyeon Lee[1] and Wooram Park[2]

Abstract— **In this paper we design a robot that can move forward and backward based on the vibration excitation. The proposed design enables the robot to locomote on the horizontal surface using the vibration excitation that is perpendicular to the locomotion direction. The bidirectional locomotion is achieved, and the direction of motion is determined by the vibration frequency. This new type of robot is useful for the unconventional environment where complex moving mechanisms cannot be applied to the robots such as medical, small pipeline, and underwater vehicle applications. To this end, two springs with different stiffness are perpendicularly connected and support the main body of the robot. The dynamic response of this nonlinear system to the vibration enables the robot to walk forward and backward depending on the vibration frequency. The numerical simulation of this system and the experiments with actual hardware design verify the proposed approach.**

I. INTRODUCTION

Nowadays it is not surprising to see robotic technologies that are applied to biology, medicine, pipe-line, and underwater environment. One of the most famous example is the robotic surgical systems [1], [2]. Usually these surgical systems consist of actuators, sensors, control system, and surgical tools. The size and complexity of the overall system are not strictly limited, but the size of the surgical tools in such systems is usually minimized for minimally invasive surgery.

The emergence of small size robots ranging from centimeters (cm) to micrometers (μm) opened the door to new types of surgery, diagnosis, and treatment. For example, let us consider endoscopy. The endoscopy is a diagnostic procedure where a doctor inserts a tethered flexible endoscope into human body to examine the interior of a hollow organ or cavity of the body. To overcome the disadvantage of the tethered endoscope (limited reachability, patient discomfort, etc.), a wireless endoscope system, or capsule endoscope, has been developed [3], [4]. In the capsule-shaped system, an optical sensor, LED light sources, image transmitter, and battery are packaged. A patient swallows the small capsule, and the system captures and transmits many images of the gastrointestinal tract for several hours. A drawback of the capsule endoscope is that it passes through the gastrointestinal tract passively by the natural peristaltic contractions of the bowel. In this way, it may miss lesions on organs. To overcome this, a couple of external actuation methods for the capsule endoscopy have been developed [5], [6], [7], and the clinical tests started very recently [8], [9]. The internal locomotion mechanisms are proposed [10], [11], [12], [13], [14], [15], [16], [17], [18], but they increase the robot size and also require an internal power source. The maneuvering methods for capsule endoscopes using magnetic field gradient or rotating magnetic field were introduced [5], [6], [7], but the study about the use of alternating (or vibrating) magnetic field is relatively rare. This paper explores the use of vibration excitation for locomotion of small robots with the hope that this technology will lead to the advancement in medical robots.

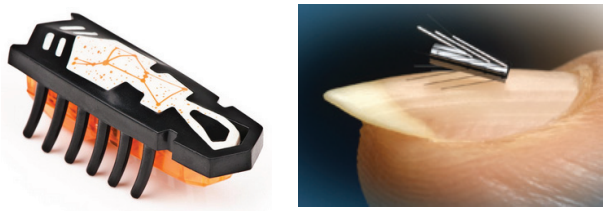

(a) (b)

Fig. 1. (a) HEXBUG toy [19]. (b) ViRob [20]

Traditionally there have been considerable efforts to reduce or avoid mechanical vibration that causes the adverse effects on the system such as part wear, loose assembly, instability, and noisy sound. However, the vibration can also cause locomotion of small robotic systems. For example, it is easily observed that when a cell phone is vibrating in the silent mode, it slides on the hard surface of a table. The vibrating mechanism of a cell phone consists of a miniature motor (about 20 mm length and 5 mm diameter) and an rotating unbalanced weight. It is surprising to realize that such a small motor can make a cell phone (over 200 g) slide without a complex mechanism such as a gearbox or wheels. In addition, the vibration of a kids' toy (Hexbug [19]) shown in Fig. 1(a) causes random style translational motion. The propulsion is generated from the physical contact between the vibrating toy legs and the ground. ViRob [20] shown in Fig. 1(b) was developed in the lab of Prof. Shoham in the Medical Robotics Laboratory at the Israel Institute of Technology in 2009, showing the possibility of the new types of medical treatment for lung cancer and cardiovascular disease. The vibrating magnetic field induces the small robot's vibration, and the robot can advance in the narrow channel due to the periodic physical interaction between the robot and the environment. Thus the vibration shows

[1]Jaeyeon Lee is with the Department of Electrical Engineering, University of Texas at Dallas, 800 W. Campbell Rd., Richardson, TX, USA.jaeyeon.lee@utdallas.edu

[2]W. Park is with the Department of Mechanical Engineering, University of Texas at Dallas, 800 W. Campbell Rd., Richardson, TX, USA.wooram.park@utdallas.edu

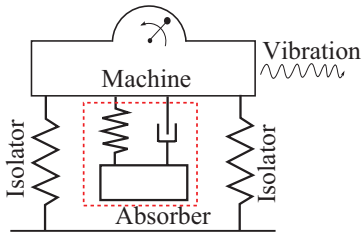

Fig. 2. Vibration absorber.

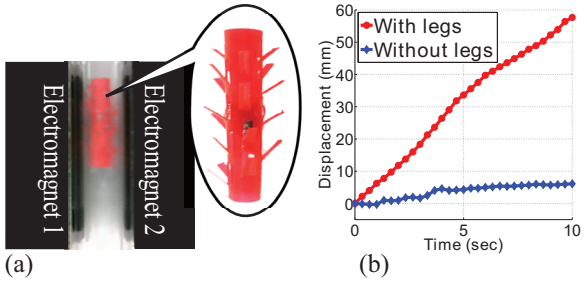

Fig. 3. (a) Vibration caterpillar robot in a pair of electromagnets. (b) Comparison between locomotions with and without legs.

two different faces, how to avoid or how to utilize. This paper is interested in how to utilize the vibration for robot locomotion.

This paper concerns the design of a robot that can move forward and backward (bidirectional locomotion) using the vibration excitation. Specifically the excitation is applied perpendicular to the locomotion direction. More importantly, the motion direction will be determined by the vibration frequency.

The main approach in this paper was inspired by vibration absorbers which is one of the traditional subjects in the vibration study. As shown in Fig. 2, the machine is operating with the internal motor or engine. This can be seen in many traditional mechanical systems such as press machines, lathes, drilling machines, and milling machines. The rotational motion of the internal actuator will also excite the system, and the vibration may induce the unwanted resonance. A vibration absorber is introduced to avoid or reduce this resonant effect. The mathematical analysis shows that we can determine the optimal parameters for the mass and the spring stiffness of the absorber so that the unwanted vibration is minimized and the vibration of the absorber is also bounded at the same time [21]. More direct use of the multi-DOF system inspired by the vibration absorber to the vibration-induced locomotion was introduced in [22]. In this work, the small-sized multi-DOF system is actuated by the vibrating plate, and the system motion can be manipulated by the various vibration input. Vartholomeos et al. [23] studied more fundamental phenomena on vibration and locomotion, and validate it by experiments. In this context, the structure design for the system becomes very important because the successful locomotion depends on the interior and exterior structure of the system.

This paper proposes a robot design which uses the vibration excitation to induce the bidirectional locomotion. This paper is organized as follows. Section II presents our preliminary tests as motivation. Section III shows our design scheme, derivation of dynamics equations and numerical analysis. In Section IV, a robot is actually built to verify the design idea and the experimental results are presented. The conclusion is given in Section V.

II. Preliminary Tests

Several preliminary tests were performed as motivation for this research. Fig. 3(a) shows a caterpillar-shape small robot which is actuated by the vibrating magnetic field. It is made of a drinking straw with the ferromagnetic metal inside, and has multiple passive legs. This small robot is placed in the plastic tube and the vibrating magnetic field is applied.

Note that the magnetic field is vibrating (or alternating), not rotating. The vibrating magnetic field is relatively easier to obtain than the rotating one by applying alternate inputs into two parallel electromagnets as shown in Fig. 3(a). To verify the effect of the legs on the caterpillar's locomotion, the caterpillar without legs was also tested. The role of the legs for the caterpillar robot was verified as shown in Fig. 3(b). The caterpillar with legs went forward, while the caterpillar without legs did not effectively walk. This locomotion was possible because of the physical interaction of the legs and the environment. The question on how to make the robot go backward still remains.

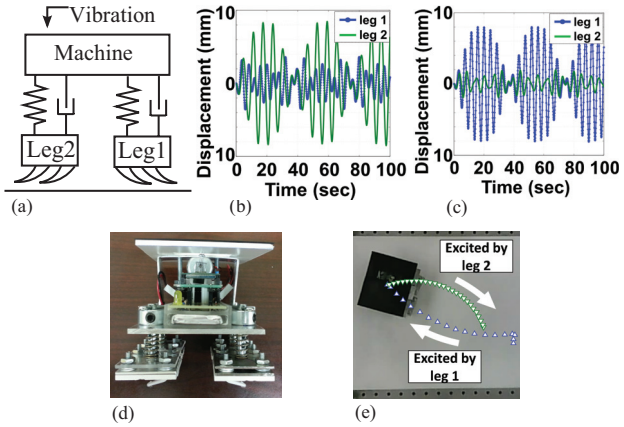

Fig. 4. (a) Design scheme of two-leg robot with vibration walking. (b) Displacement of the legs with low frequency vibration. (c) Displacement of the legs with high frequency vibration. (d) Hardware implementation. (e) Bidirectional locomotion.

Fig. 4 shows the test with a fist-size robot for bidirectional locomotion induced by different vibration frequencies. This prototype was inspired by the fact that the dynamic response of the vibration absorber is different depending on the vibration frequency. This opens a way to control a vibrating robot by changing the vibration frequency. Fig. 4(a) shows the design scheme of the two-leg walking robot. In the main machine, the motor with the unbalanced weight generates the vibration. By employing a hard spring on the left and a soft one on the other, we can obtain the different vibration

responses from the two legs. Due to the special design of the bottom surface of the foot, the physical collision between the foot and the ground induces the translational motion of the system. In Figs. 4(b) and (c), the numerical simulation shows that the legs are intrinsically fluctuated depending on the vibration frequency. Consequently by changing the vibration frequency, we can obtain the locomotion in the opposite direction. Based on the design scheme, we made the hardware as shown in Fig. 4(d) and the robot moved bidirectionally depending on the vibration frequency as shown in Fig. 4(e) in which the triangles denote the positions of the robot center captured in video at every time step $\Delta t = 0.33s$.

III. Design, Mathematical Model, and Numerical Analysis

The design for the robot in this paper is directly inspired by the work in [23]. The main difference is that the horizontal force by the unbalanced weight is ignored and only vertical excitation is considered. We apply multiple springs so as to induce the bidirectional locomotion using vibration with multiple input frequencies. A large block (mass M) is connected to a foot (mass m) through two spring-damper sets as shown in Fig. 5(a). Some assumptions employed for the mathematical model are as follow.

- This model is in 2D space.
- Upper block (M) does not rotate.
- Foot (m) is always in contact with the ground.
- We ignore the horizontal vibration force.
- Coulomb friction model is used for horizontal friction force between the foot and the ground.
- The spring and damper are linear and massless.
- The hinge is frictionless.

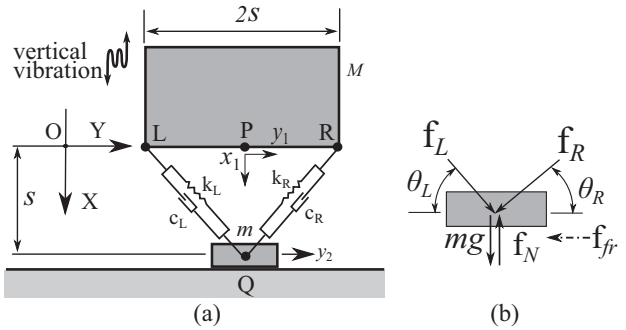

Fig. 5. (a) The proposed design (b) Free body diagram for the foot

The block and the foot can move by (x_1, y_1) and $(0, y_2)$, respectively. The absolute position of the three points (L,R,Q) are expressed as $OL = (x_1, y_1 - s)$, $OR = (x_1, y_1 + s)$, and $OQ = (s, y_2)$. The spring constants are k_L and k_R, and the damping constants are c_L and c_R.

For a simple model, we prevent the rotational motion of the large block. This assumption becomes obvious if two sets of a foot and two springs are horizontally attached under the large block. The actual implementation of the hardware will use four foot sets, each of which consists of a foot and two springs to ensure the balance as will be shown in Section IV, but its theoretical analysis can be done with the reduced system shown in Fig. 5(a).

Fig. 5(b) shows the free-body diagram for the foot. The sum of the spring force and the damping force is given as

$$f_L = k_L(s\sqrt{2} - \sqrt{(x_1 - s)^2 + (y_1 - y_2 - s)^2}) - c_L \frac{(x_1 - s)\dot{x}_1 + (y_1 - y_2 - s)(\dot{y}_1 - \dot{y}_2)}{\sqrt{(x_1 - s)^2 + (y_1 - y_2 - s)^2}}$$

and

$$f_R = k_R(s\sqrt{2} - \sqrt{(x_1 - s)^2 + (y_1 - y_2 + s)^2}) - c_R \frac{(x_1 - s)\dot{x}_1 + (y_1 - y_2 + s)(\dot{y}_1 - \dot{y}_2)}{\sqrt{(x_1 - s)^2 + (y_1 - y_2 + s)^2}}.$$

In geometry, the angles are computed as

$$\theta_L = \tan^{-1}(|x_1 - s|/|y_1 - y_2 - s|)$$
$$\theta_R = \tan^{-1}(|x_1 - s|/|y_1 - y_2 + s|)$$

Since we assume that the foot is always in contact with the ground, we have the force equilibrium as

$$f_L \sin(\theta_L) + f_R \sin(\theta_R) + mg - f_N = 0.$$

We have the motion equation for the foot as

$$m\ddot{y}_2 = f_y - f_{fr} \quad (1)$$

where the force f_y is defined as $f_y = f_L \cos(\theta_L) - f_R \cos(\theta_R)$, and f_{fr} is the friction force. When the viscous friction is ignored, the maximum friction f_C is given as $f_C = \mu f_N$ where μ is the coefficient of friction. The friction force f_{fr} is computed as

$$f_{fr} = \begin{cases} f_C\, sgn(\dot{y}_2), & \text{if } \dot{y}_2 \neq 0 \\ f_y, & \text{if } \dot{y}_2 = 0 \text{ and } |f_y| <= f_C \\ f_C\, sgn(f_y), & \text{if } \dot{y}_2 = 0 \text{ and } |f_y| > f_C. \end{cases}$$

We assume that vertical vibration is induced by a rotating unbalanced weight (m_s) on the block. The equations of motion are written as

$$M\ddot{x}_1 = Mg - f_L \sin(\theta_L) - f_R \sin(\theta_R) + m_s r\omega^2 \cos\omega t \quad (2)$$
$$M\ddot{y}_1 = f_R \cos(\theta_R) - f_L \cos(\theta_L) \quad (3)$$

where ω is the angular velocity of the unbalanced weight and r is the distance of the unbalanced weight from the rotation center.

As aforementioned, we consider the vertical vibration and ignore the horizonal effect of the rotating unbalanced weight. This will be implemented in the hardware design by rotating the weight on the $x-z$ plane (see Fig. 5(a)). The main reason we focus on this type of vibration is because in this paper we are testing the idea that the vibration excitation perpendicular to the locomotion direction can induce the locomotion. We performed the numerical simulation for the design using the equations of motion in (1)-(3). The system parameters are given in Table I. The vibration frequencies 4Hz and 7Hz were tested. Although we chose these two vibration frequencies

TABLE I

SYSTEM PARAMETERS FOR NUMERICAL SIMULATION

$M(kg)$	$m(kg)$	$m_s(kg)$	μ	$s(m)$
0.3	0.01	0.04	0.176	0.05
$c_L(Nsec/m)$	$c_R(Nsec/m)$	$k_L(N/m)$	$k_R(N/m)$	$r(m)$
2.5	2.5	400	300	0.02

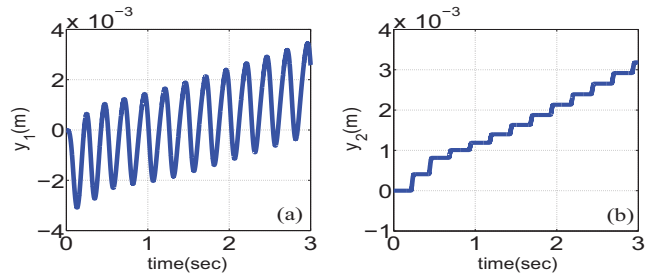

Fig. 6. Simulation result for robot locomotion with the vibration frequency 4Hz. The robot is moving to the +y direction. (a) Horizontal position of the large block. (b) Horizontal position of the foot.

by trial-and-error, the starting point for the frequency search was obtained as follows. The locomotion will be driven by the resonance effect in each spring. The natural frequency of the vertical motion of the large block can be estimated by $f = \sqrt{k_c}/(2\pi\sqrt{M})$ where k_c is the combined spring constant of the two springs for the vertical direction as $k_c = (k_L + k_R)/\sqrt{2}$. The frequency is computed as $f = 6.5$Hz. Using this starting point, we chose the two frequencies 4Hz and 7Hz for the simulation tests.

Fig. 6 shows the results from numerical simulation with the vibration frequency 4Hz. The robot is moving to the right (+y direction). It is worth seeing the horizontal net force ($\ddot{y_2}$) computed in (1) shown in Fig. 7. Even though the vibration excitation is applied in the vertical direction, the asymmetric horizontal force is generated on the foot due to the asymmetry of the two springs and the surface friction.

Fig. 8 shows the lengths of the two springs in the test with the frequency 4Hz. The right spring (softer than the left one) has higher fluctuation than the left one. We can expect that this will change with the different vibration frequency, which may lead to the locomotion to the opposite direction. The last thing to check is the normal force f_N on the foot. Since we

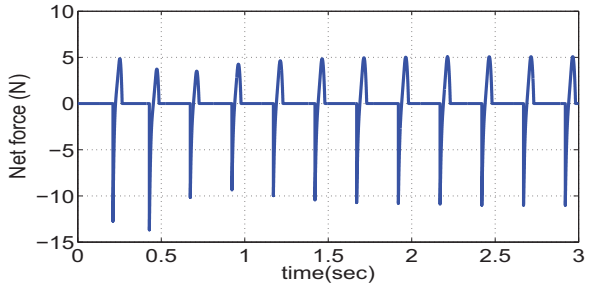

Fig. 7. Simulation result for horizontal net force on the foot with the vibration frequency 4Hz.

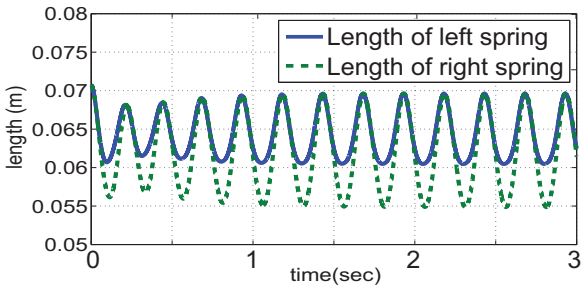

Fig. 8. Lengths of springs with the vibration frequency 4Hz.

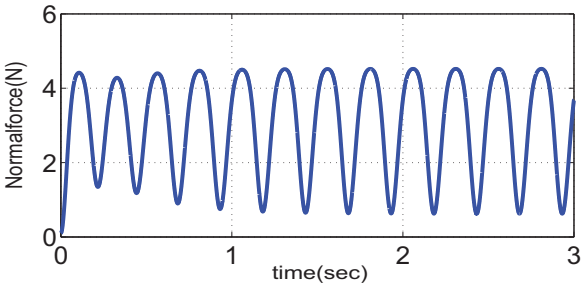

Fig. 9. The normal force on the foot when the vibration frequency is 4Hz.

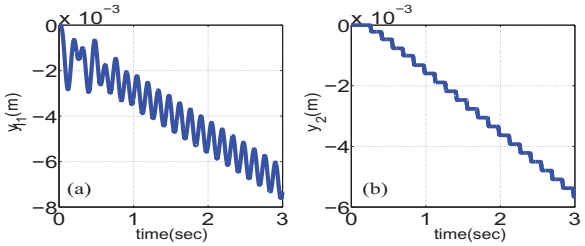

Fig. 10. Simulation result for robot locomotion with the vibration frequency 7Hz. The robot is moving to the -y direction. (a) Horizontal position of the large block. (b) Horizontal position of the foot.

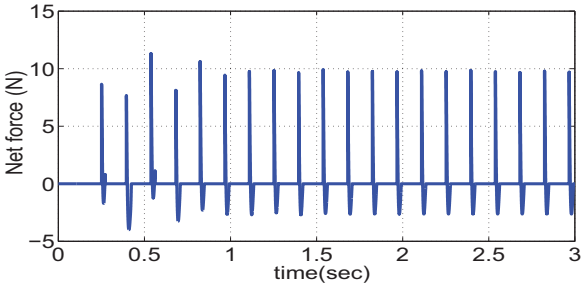

Fig. 11. Simulation result for horizontal net force on the foot with the vibration frequency 7Hz.

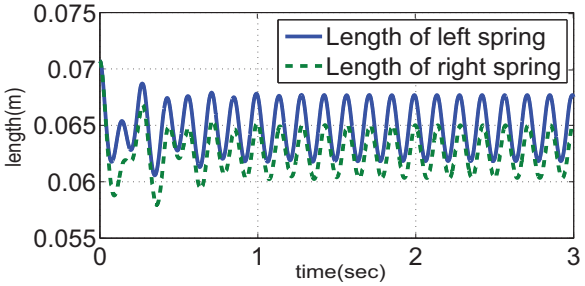

Fig. 12. Lengths of springs with the vibration frequency 7Hz.

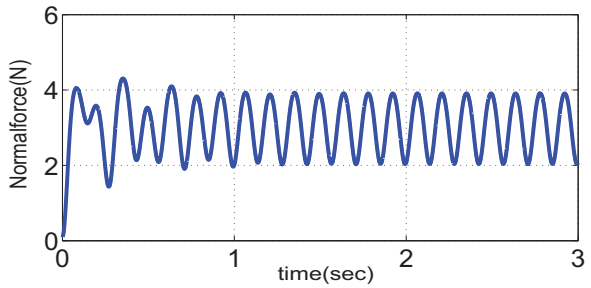

Fig. 13. The normal force on the foot when the vibration frequency is 7Hz.

assumed that the contact between the foot and the ground is preserved, we should check if the normal force is always positive. Fig. 9 confirms that the normal force is positive when the vibration frequency is 4Hz.

With the vibration frequency 7Hz, the robot moves to the left (-y direction) as shown in Fig. 10. Fig. 11 shows the horizontal net force ($\ddot{y}_2$) on the foot. With the vibration frequency 7Hz, the left spring (stiffer than the right one) fluctuates more than the right one as shown in Fig. 12. Fig. 13 confirms that the normal force is always positive when the vibration frequency is 7Hz.

Through the numerical analysis, we confirmed the possibility that the proposed design can move forward and backward directions, and the direction is determined by the specific vibration frequencies.

IV. Hardware Implementation and Experiments

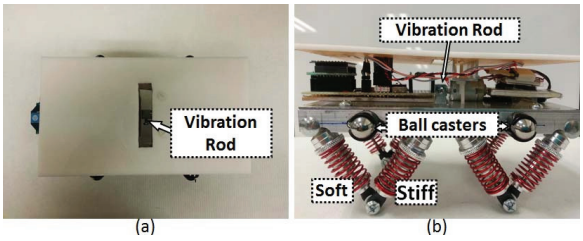

Fig. 14. Robot system. (a) Top view (b) Side view.

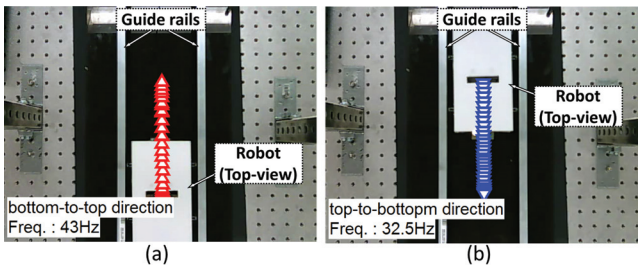

Fig. 15. Experiment results. (a) Locomotion with 43Hz vibration. (b) Locomotion with 32.5Hz vibration.

To verify the design idea proposed in this paper, we built the robot according to the design and performed the experiments.

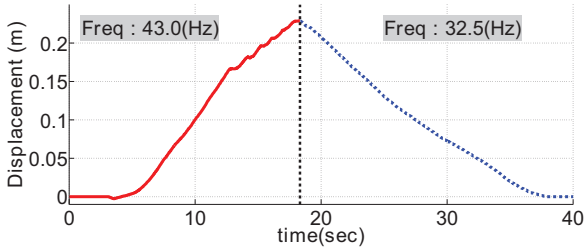

Fig. 16. Location of the robot.

TABLE II
System Parameters for Each Unit of the Hardware

$M(kg)$	$m(kg)$	$m_s(kg)$	μ
0.071	0.007	0.013	0.176
$s(m)$	$k_L(N/m)$	$k_R(N/m)$	$r(m)$
0.08	1740	955	0.011

A. Hardware

The small robot we designed is shown in Fig. 14. To ensure the balance of the whole system on the horizon ground, we built the small robot by combining four simplified unit as proposed in Fig. 5(a). Each unit consists of a foot, a stiff spring and a soft spring. We used shock absorbers that are generally used in RC cars. A round metal plate is assembled at end of each leg as a foot. A motor to generate vibration frequency was attached to the center of the robot body and its frequency was controlled wirelessly. The experimental parameters for each unit are given in Table II. Note that we do not have to specify the damping constants, because the dampers are used to guarantee the stability and they do not affect the special frequencies that induce the bidirectional locomotion. As explained in Section III, the rotation plane of the unbalanced weight is perpendicular to the locomotion direction. To prevent the motion along z-axis (see Fig. 5(a)) the guide rails are used as shown in Fig. 15. Ball casters attached on both sides of the robot ensure the smooth slide of the robot on the guide rails. The total robot size is 90 mm(L)$\times$ 160 mm(W) $\times$95 mm(H) and the total weight is 0.502 kg.

B. Experiments

Experiments were performed by putting the robot between two parallel guide rails which help the robot to move in two directions (forward or backward) and one web camera is mounted above the robot perpendicularly to capture the motion of the robot. According to theory, the robot was expected to move to the side of stiff springs with relatively high vibration frequency and will move to the opposite direction with relatively low frequency.

As explained in Section III, we computed the starting point for the frequency search. The combined spring constant for the robot along the vertical direction was measured as $k_c = 3458.8$ N/m. This measured spring constant is slightly larger than the combined spring constant calculated by parameters in Table II. Since the body mass is M = 0.071 kg, the natural frequency is $\sqrt{k_c}/(2\pi\sqrt{M}) = 35.1$Hz. From

this value, we tested with various frequencies. After trial and error, we chose the frequencies 43Hz and 32.5Hz for the test.

Fig. 15 shows the experimental results captured by the web camera. The triangles denote the positions of the robot center captured in video at every time step $\Delta t = 0.67s$. As shown in Fig. 15(a), the robot moves upward (to stiff springs) when the vibration frequency is 43Hz. With the frequency 32.5Hz, the downward locomotion (to soft springs) was observed as shown in Fig. 15(b). Fig. 16 shows the plot of the robot position as a function of time. This test was performed continuously. In other words, the vibration frequency was changed from 43Hz to 32.5Hz at t=18(sec). With this frequency change, the locomotion direction was promptly changed.

For the actual experiments, we used different design parameters from the numerical analysis in Section III because the parameters in the numerical analysis are not realizable. For example, the actual small robot generally excited by the vibration frequency at least 30Hz. Above all, the purpose of the numerical analysis is not to find a specific frequency for the bidirectional motion but to confirm the possibility for the bidirectional motion.

V. CONCLUSIONS

In this paper, we proposed a design for a robot that could move forward and backward using the vibration excitation of two different frequencies. Asymmetric spring supports were used in the robot design. To verify the design idea, we performed a numerical simulation, and then implemented our design by making a test robot.

Due to the asymmetry of springs and the surface friction between the robot and the ground, the asymmetric horizontal force was produced from the vertical vibration. This force generated the locomotion of the robot. Using the vibration frequency, we could control the direction of the robot locomotion. We verified the manipulation of robot locomotion by changing vibration frequency in the numerical simulation and the actual experiments.

The proposed design idea opens a door to new design scheme for medical devices such as a capsule endoscope and micro medical robots. Since the size of the medical robots is strictly limited, the internal actuation is hard to apply. However, it is relatively easy to excite the small robot using vibrating magnetic field. If we adapt the design method proposed in this paper to the design of medical robots, it becomes possible to manipulate them using remote magnetic field. The surface design and fabrication for this system in micro or nano scale will be a challenging research topic for the future.

REFERENCES

[1] G. H. Ballantyne and F. Moll, "The da vinci telerobotic surgical system: the virtual operative field and telepresence surgery," *Surgical Clinics of North America*, vol. 83, no. 6, pp. 1293–1304, 2003.

[2] A. D. Pearle, D. Kendoff, V. Stueber, V. Musahl, and J. A. Repicci, "Perioperative management of unicompartmental knee arthroplasty using the mako robotic arm system (makoplasty)," *Am J Orthop (Belle Mead NJ)*, vol. 38, no. 2 Suppl, pp. 16–19, 2009.

[3] G. Eisen, R. Eliakim, A. Zaman, J. Schwartz, D. Faigel, E. Rondonotti, F. Villa, E. Weizman, K. Yassin *et al.*, "The accuracy of pillcam eso capsule endoscopy versus conventional upper endoscopy for the diagnosis of esophageal varices: a prospective three-center pilot study," *Endoscopy*, vol. 38, no. 01, pp. 31–35, 2006.

[4] C. Gheorghe, R. Iacob, I. Bancila *et al.*, "Olympus capsule endoscopy for small bowel examination," *Journal of Gastrointestinal and Liver Diseases*, vol. 16, no. 3, p. 309, 2007.

[5] G. Kósa, P. Jakab, F. Jólesz, and N. Hata, "Swimming capsule endoscope using static and rf magnetic field of mri for propulsion," in *Robotics and Automation, 2008. ICRA 2008. IEEE International Conference on*. IEEE, 2008, pp. 2922–2927.

[6] M. Sendoh, K. Ishiyama, and K.-I. Arai, "Fabrication of magnetic actuator for use in a capsule endoscope," *Magnetics, IEEE Transactions on*, vol. 39, no. 5, pp. 3232–3234, 2003.

[7] H. Keller, A. Juloski, H. Kawano, M. Bechtold, A. Kimura, H. Takizawa, and R. Kuth, "Method for navigation and control of a magnetically guided capsule endoscope in the human stomach," in *Biomedical Robotics and Biomechatronics (BioRob), 2012 4th IEEE RAS & EMBS International Conference on*. IEEE, 2012, pp. 859–865.

[8] P. Swain, A. Toor, F. Volke, J. Keller, J. Gerber, E. Rabinovitz, and R. I. Rothstein, "Remote magnetic manipulation of a wireless capsule endoscope in the esophagus and stomach of humans," *Gastrointestinal endoscopy*, vol. 71, no. 7, pp. 1290–1293, 2010.

[9] J. Rey, H. Ogata, N. Hosoe, K. Ohtsuka, N. Ogata, K. Ikeda, H. Aihara, I. Pangtay, T. Hibi, S. Kudo *et al.*, "Feasibility of stomach exploration with a guided capsule endoscope," *Endoscopy*, vol. 42, no. 07, pp. 541–545, 2010.

[10] R. Carta, M. Sfakiotakis, N. Pateromichelakis, J. Thoné, D. Tsakiris, and R. Puers, "A multi-coil inductive powering system for an endoscopic capsule with vibratory actuation," *Sensors and Actuators A: Physical*, vol. 172, no. 1, pp. 253–258, 2011.

[11] C. Quaglia, E. Buselli, R. J. Webster III, P. Valdastri, A. Menciassi, and P. Dario, "An endoscopic capsule robot: a meso-scale engineering case study," *Journal of Micromechanics and Microengineering*, vol. 19, no. 10, p. 105007, 2009.

[12] S. Park, H. Park, S. Park, and B. Kim, "A paddling based locomotive mechanism for capsule endoscopes," *Journal of mechanical science and technology*, vol. 20, no. 7, pp. 1012–1018, 2006.

[13] W. Li, W. Guo, M. Li, and Y. Zhu, "A novel locomotion principle for endoscopic robot," in *Mechatronics and Automation, Proceedings of the 2006 IEEE International Conference on*. IEEE, 2006, pp. 1658–1662.

[14] M. E. Karagozler, E. Cheung, J. Kwon, and M. Sitti, "Miniature endoscopic capsule robot using biomimetic micro-patterned adhesives," in *Biomedical Robotics and Biomechatronics, 2006. BioRob 2006. The First IEEE/RAS-EMBS International Conference on*. IEEE, 2006, pp. 105–111.

[15] S. Guo, Y. Ge, L. Li, and S. Liu, "Underwater swimming micro robot using ipmc actuator," in *Mechatronics and Automation, Proceedings of the 2006 IEEE International Conference on*. IEEE, 2006, pp. 249–254.

[16] R. Carta, G. Tortora, J. Thoné, B. Lenaerts, P. Valdastri, A. Menciassi, P. Dario, and R. Puers, "Wireless powering for a self-propelled and steerable endoscopic capsule for stomach inspection," *Biosensors and Bioelectronics*, vol. 25, no. 4, pp. 845–851, 2009.

[17] P. Glass, E. Cheung, and M. Sitti, "A legged anchoring mechanism for capsule endoscopes using micropatterned adhesives," *Biomedical Engineering, IEEE Transactions on*, vol. 55, no. 12, pp. 2759–2767, 2008.

[18] S. Tognarelli, C. Quaglia, P. Valdastri, E. Susilo, A. Menciassi, and P. Dario, "Innovative stopping mechanism for esophageal wireless capsular endoscopy," *Procedia Chemistry*, vol. 1, no. 1, pp. 485–488, 2009.

[19] Hexbug, "Hexbug nano," `http://www.hexbug.com/`.

[20] Microbotmedical, "Virob," `http://www.microbotmedical.com/`.

[21] S. S. Rao, *Mechanical Vibrations, 4th edition*. Pearson Education India, 2003.

[22] T. Yasuda, I. Shimoyama, and H. Miura, "Microrobot actuated by a vibration energy field," *Sensors and Actuators A: Physical*, vol. 43, no. 1, pp. 366–370, 1994.

[23] P. Vartholomeos and E. Papadopoulos, "Dynamics, design and simulation of a novel microrobotic platform employing vibration microactuators," *J. of Dynamics System, Measurement and Control*, vol. 128, pp. 122–133, 2006.